DEVELOPMENT OF SUBCHANNEL VOID MEASUREMENT SENSOR AND MULTIDIMENSIONAL TWO-PHASE FLOW DYNAMICS IN ROD BUNDLE

T. Arai¹, M. Furuya¹, T. Kanai¹, K. Shirakawa¹
¹ Central Research Institute of Electric Power Industry, Tokyo, Japan

Abstract

An accurate subchannel database is crucial for modeling the multidimensional two-phase flow in a rod bundle and for validating subchannel analysis codes. Based on available reference, it can be said that a point-measurement sensor for acquiring void fractions and bubble velocity distributions do not infer interactions of the subchannel flow dynamics, such as a cross flow and flow distribution, etc. In order to acquire multidimensional two-phase flow in a 10×10 rod bundle with an o.d. of 10 mm and 3110 mm length, a new sensor consisting of 11-wire by 11-wire and 10-rod by 10-rod electrodes was developed. Electric potential in the proximity region between two wires creates a void fraction in the center subchannel region, like a so-called wire mesh sensor. A unique aspect of the devised sensor is that the void fraction near the rod surface can be estimated from the electric potential in the proximity region between one wire and one rod. The additional 400 points of void fraction and phasic velocity in 10×10 bundle can therefore be acquired. The devised sensor exhibits the quasi three-dimensional flow structures, i.e. void fraction, phasic velocity and bubble chord length distributions. These quasi three-dimensional structures exhibit the complexity of two-phase flow dynamics, such as coalescence and the breakup of bubbles in transient phasic velocity distributions.

Introduction

In a boiling water reactor (BWR), fuel rod bundles have been developed to improve heat removal performance to improve economic efficiency and reliability. The diameter of the fuel cladding tube has decreased, and the design of the spacer has also been modified (such as by attaching a mixing vane to the spacer to enhance the critical heat flux). In order to highly optimize the configuration of the rod bundle, it is important to clarify the multi-dimensional two-phase flow dynamics in a complicated rod bundle flow channel.

With the development of numerical calculation technology in recent years, multi-dimensional two-phase flow analysis codes (such as subchannel analysis) and computational fluid dynamics (CFD) have been applied to rod bundle geometry. When focusing on the rod bundle geometry, especially in the subchannel, there are a variety of physical models both of the micro scale and macro scale in the two-phase flow.

The multidimensional two-phase flow needs to be theoretically-modelled on the basis of the dominant physical phenomena. Therefore, an accurate subchannel database is crucial for modelling the multidimensional two-phase flow in a rod bundle and validation of these analysis codes.

The conventional experimental research used to clarify the mechanism of two-phase flow and obtain the validation data is as follows. Sadatomi et al. [1] conducted an air-water two-phase flow experiment using 2×3 rod bundle test sections, and evaluated the drift flow (cross flow) between

subchannels. The existing correlation equation has been validated by the experimental results; void fraction, bubble velocity, pressure loss in each subchannel measured by a needle probe. With respect to discrimination of the flow regime in the bundle flow channel, Mizutani et al. [2] conducted an airwater two-phase flow experiment using the transparent test channel with a 4×4 rod bundle geometry, and observed the two-phase flow behaviour in each sub-channel with a fiberscope and high-speed digital video camera. The experimental results indicate that the flow regime in each subchannel is divided into bubbly flow, the transition region from bubbly flow to churn flow, churn flow, and annular flow. Paranjape et al. [3] performed void measurements using a 4-sensor probe in the airwater two-phase flow experiment with an 8×8 rod bundle flow channel. The void fraction, gas velocity, sauter mean diameter of bubbles, and interfacial area concentrations were evaluated in each subchannel. These results show that the two-phase flow dynamics in the center subchannel region differ from those in the rod gap. According to the steam-water two-phase flow in high-temperature and high-pressure conditions, Nuclear Power Engineering Corporation (NUPEC) [4] conducted a thermal-hydraulics test (opened to the public as the BFBT project) in which a time-averaged void fraction distribution is measured by X-ray CT across the full size 8×8 rod bundle geometry.

However, several technical subjects within the detailed mechanism of two-phase flow in a complicated flow channel like a subchannel have not yet been clarified. One of these is the discrimination of flow regime and flow transition. In the case of vertical upward two-phase flow, the flow regime is mainly classified into bubbly flow, slug flow, churn flow and annular flow. Since the flow regime is distinguished by the flow conditions and flow channel geometry, it is necessary to evaluate the effects of cross flow, coalescence and breakup of bubbles, etc. The other subject is the three-dimensional distribution of the two-phase flow structure. Even if the flow regime or flow conditions are the same, the differences between the flow channel geometry and spacer configuration can affect not only drift and turbulent flow dynamics, but also the heat transfer characteristics of the rod bundle.

Most existing experiments have acquired information as one-point or time-averaged two-phase flow distributions. In order to clarify the technical subjects shown above, it is important to obtain time series data in each subchannel, and to evaluate the multidimensional two-phase flow dynamics in each subchannel. The objectives of this study are to develop a high-speed and three-dimensional measuring technique for the two-phase flow in each subchannel, and to evaluate the applicability of this technique to the three-dimensional two-phase flow dynamics in the rod bundle using the air-water two-phase flow experiment.

1. Development of subchannel void sensor (SCVS)

1.1 Design of sensor

Figure 1 is a schematic diagram of a SubChannel Void Sensor (SCVS). In order to measure the void fraction at a high-sampling rate in all of the subchannels in the rod bundle, SCVS measures the local conductance between electrodes at a high sampling rate. The design of SCVS was based on the 10×10 rod bundle geometry. The outer diameter of the rod was 10 mm, and rod pitch was 13 mm. 11-wires by 11-wires were inserted in the gaps between the rods, and acted as electrodes. 11 wires of both layers crossed at 90° with a gap of 2 mm. The diameter of the wires was 0.2 mm. The electric potential at the cross point of one wire with another created the local void fraction in the center subchannel region, e.g., 121 points (= 11×11) of the void fraction distribution.

A unique feature of the devised sensor was that the void fraction near rod surface could be estimated using the electric potential in the proximity region of one wire from one rod. The simulated fuel rods were used as independent electrodes. The electric potential at the proximity region of one wire and one rod gave the local void fraction on the surface of the rod, e.g., 400 points (= $10 \times 10 \times 4$) of the void fraction distribution. Therefore, the sensor was able to measure 512 points of the local void fraction in the center subchannel and the surface of rod in a 10×10 rod bundle flow channel.

1.2 Measurement principle

The signal processing of the SCVS was based on the signal processing of the wire-mesh sensor (WMS) system. WMS is a void sensor consisting of a pair of parallel wire layers located at the cross section of a pipe [5]. Both of the parallel wires cross at 90° with a small gap. WMS can measure the void fraction distribution, phasic velocity distribution, bubble diameter distribution, and interfacial area concentration distribution at the cross section of the pipe [6]-[8]. The experimental data has been compared with other two-phase flow measuring techniques such as the needle probe and X-ray Tomography [9], [10]. WMS has been applied not only to air-water two-phase flow under atmospheric pressure conditions but also steam-water two-phase flow under high-temperature and high-pressure conditions [11]. Since the final objective of the devised SCVS was also to apply the steam-water two-phase flow measurement under high-temperature and high-pressure conditions equivalent to BWR conditions, the signal processing of the WMS system was applied to the SCVS

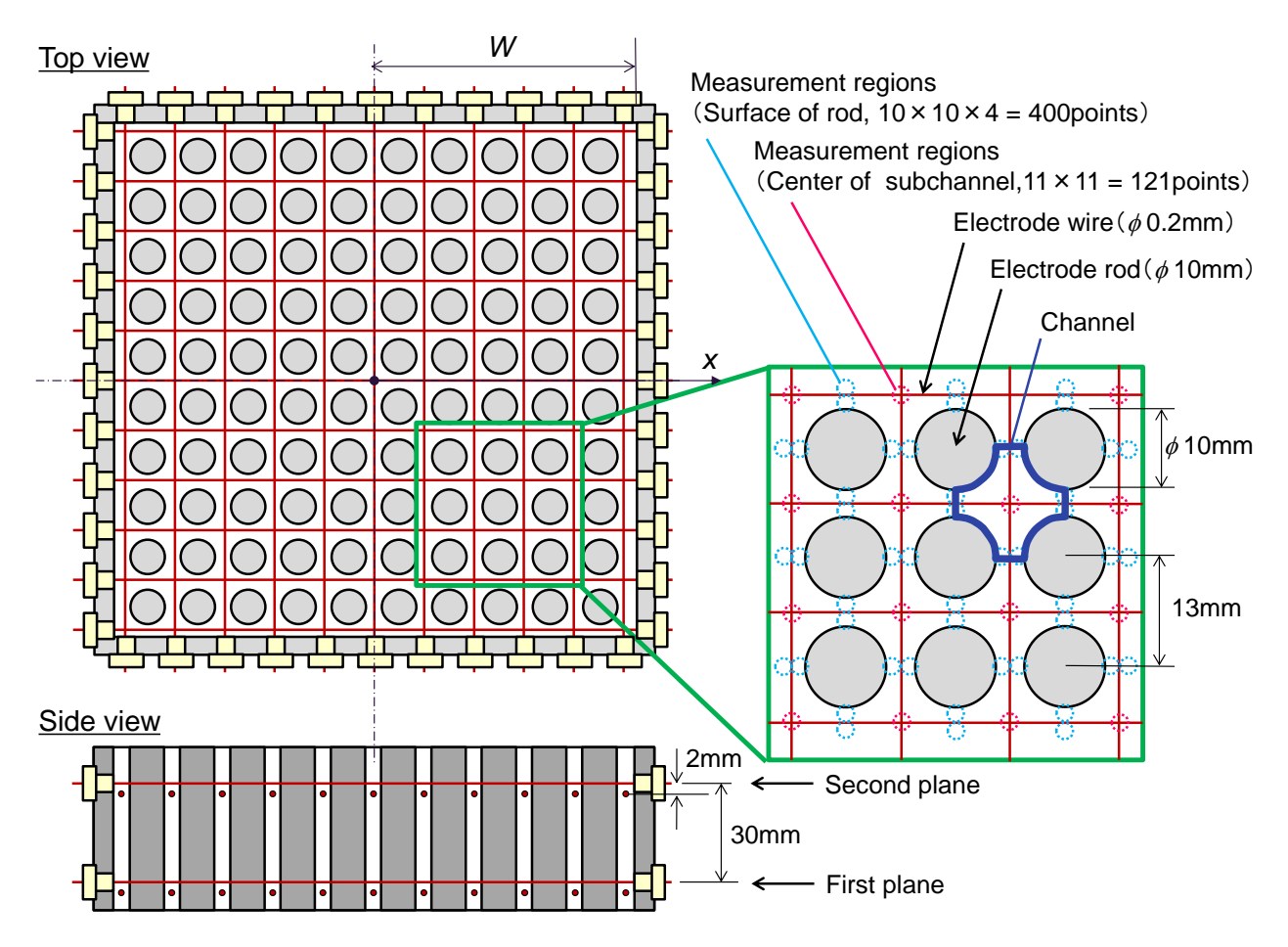


Figure 1 Schematic of subchannel void sensor

SCVS has two kinds of measuring systems with a combination of an excited electrode and measured electrode. One is the combination of two layers of wire electrodes; the measurement region is the center subchannel. The other is the combination of a wire electrode and a rod electrode; the measurement region is the surface of the rod. Figure 2 shows a schematic of the measurement principle in each measuring system. Figure 2(a) shows an example of signal processing measuring in the center subchannel region. One layer of the parallel wires works as an excited electrode, and the other works as a measured electrode. When switch S1 is closed, an excitation pulse is supplied to electrode E1. The pulse is excited as a bipolar rectangular wave to the base potential, which is referred to the rest potential of the electrode in water. An electric potential is acquired by each measured electrode, and one-dimensional void fraction distribution along the E1 is estimated by converting the electric potential into a void fraction. By switching the S1-S4 switches, twodimensional void fraction distribution at the center subchannel region is acquired. During the void measurement, the electric potential of all the simulated fuel rods is held at the rest potential of the measured electrode in water in order to reduce crosstalk between neighbouring measured electrodes. Figure 2(b) shows an example of signal processing measuring at the surface of a simulated fuel rod. The rods work as excited electrodes, and the grid of wires work as measured electrodes. When switch S1 is closed, the excitation pulse is supplied to electrode E1. An electric potential is acquired by each measured electrode, and a circumferential void fraction distribution on the surface of electrode E1 is acquired by converting the electric potential into a void fraction. By switching S1-S9, two-dimensional void fraction distribution at the rod surface is acquired.

Electric potential U(t) acquired by SCVS estimates the local void fraction $\alpha(t)$ according to the following equation based on the electric potentials at single-phase liquid and single-phase gas.

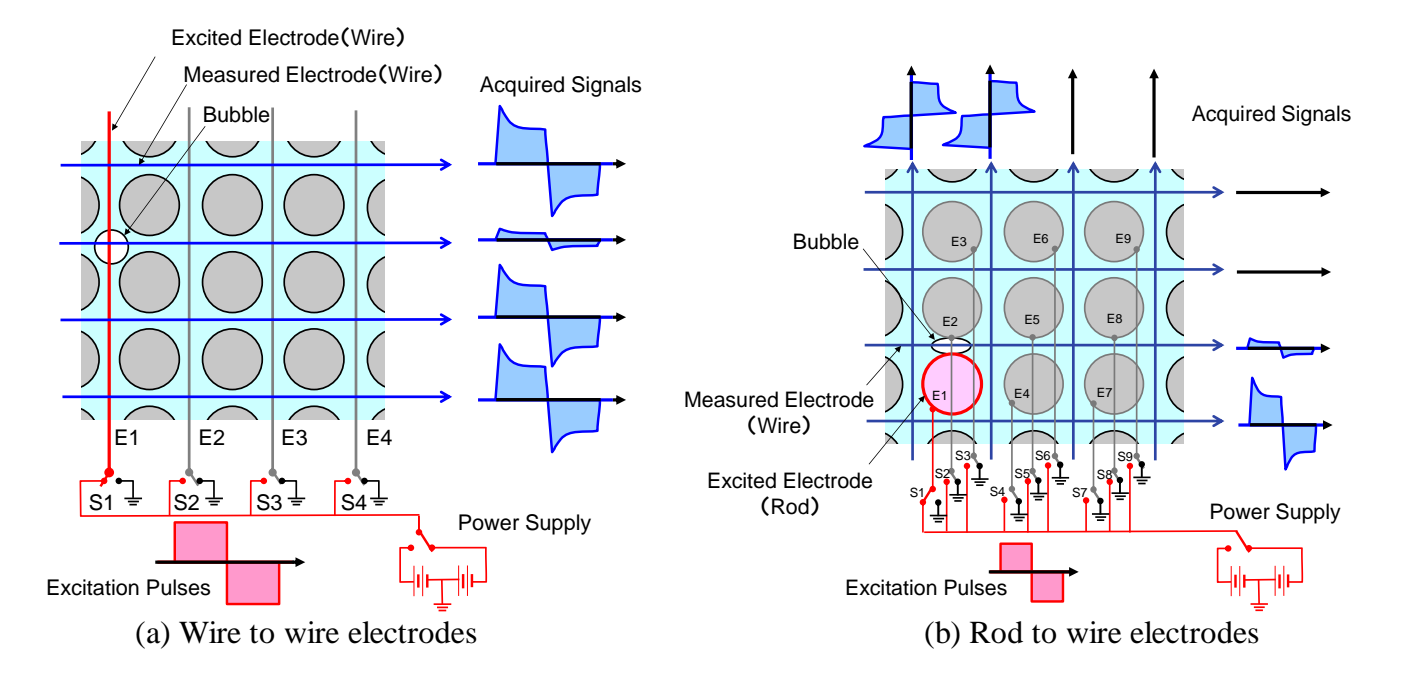


Figure 2 Measurement principle of SCVS

$$\alpha(t) = \frac{U_{water} - U(t)}{U_{water} - U_{air}} = 1 - \frac{U(t)}{U_{water}}$$
(1)

where U_{water} is the electric potential in single-phase water, and U_{air} is the electric potential in single-phase air. Since the electric potential in single-phase air is usually zero, U_{air} is negligible.

1.3 Evaluation of phasic velocity

Phasic velocity is the moving velocity of the gas-liquid interface. The phasic velocity was evaluated by a pair of time series data from the void fractions obtained by the sensors. The pair of sensors were mounted 30 mm apart from each other in the axial direction. When a bubble passes the pair of sensors, there is a time lag between the sensors. The one-dimensional phasic velocity in the axial direction is calculated as:

$$u_g = \frac{s}{\tau_t} \tag{2}$$

where s is the distance between the sensors, s is 30mm in this experiment, and τ_t is a time lag when the bubbles pass through the pair of sensors.

 τ_l is calculated by cross correlation analysis of the time series data of local void fraction at the same axial position obtained by a pair of sensors. The time lag at the maximum cross-correlation coefficient is defined as τ . The cross-correlation coefficient R_{fg} is calculated using following equation:

$$R_{fg}(\varphi) = \frac{\int_{a}^{b} \{f(t) - \overline{f}\} \{g(t + \varphi) - \overline{g}\} dt}{\sqrt{\int_{a}^{b} \{f(t) - \overline{f}\}^{2}} dt \sqrt{\int_{a}^{b} \{g(t + \varphi) - \overline{g}\}^{2}} dt}$$
(3)

where f(t) is the measurement signal of the first plane sensor and g(t) is the measurement signal of the

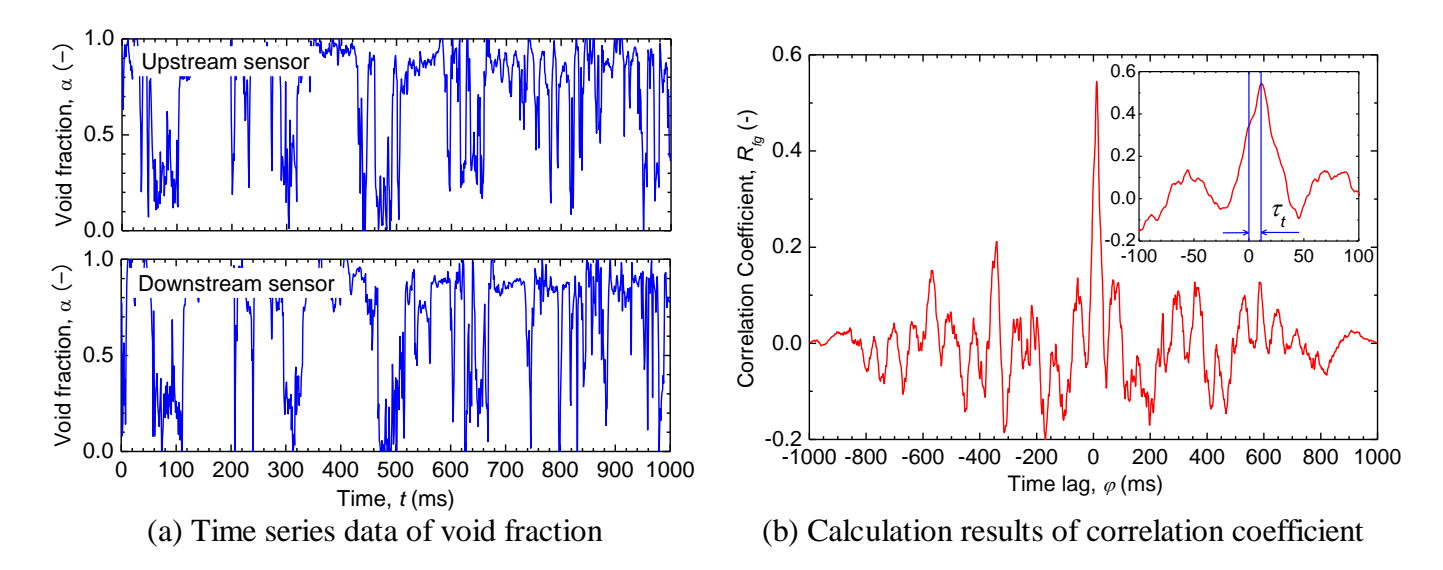


Figure 3 Evaluation of time lag between sensors

second plane sensor. Figure 3 shows the calculation results of the time lag determined by the maximum of the cross correlation coefficient. Figure 3(a) is a pair of the time series data of void fractions in the same axial position as the sensors. As shown in Figure 3(b), the time lag τ_t is determined as 11ms, and the phasic velocity is estimated as 2.7 m/s.

1.4 Evaluation of bubble chord length

The bubble chord length is the one-dimensional axial length of bubble, and it is an index of bubble size. The bubble chord length can be evaluated by time series data of the local void fraction obtained by a pair of sensors. The bubble chord length is calculated as:

$$l_{g} = u_{g} \tau_{g} \tag{4}$$

where τ_g is the residence time when a bubble passes through the sensor plane. Figure 4 shows the calculation result of the residence time of each bubble. The original time series data is binarized by a certain threshold. The threshold of the binary processing is implicitly determined so that the time-averaged void fraction of the original data is equal to that of the binarized data. The bubble chord length distribution was acquired by counting all the bubbles that pass the sensor within the measurement time.

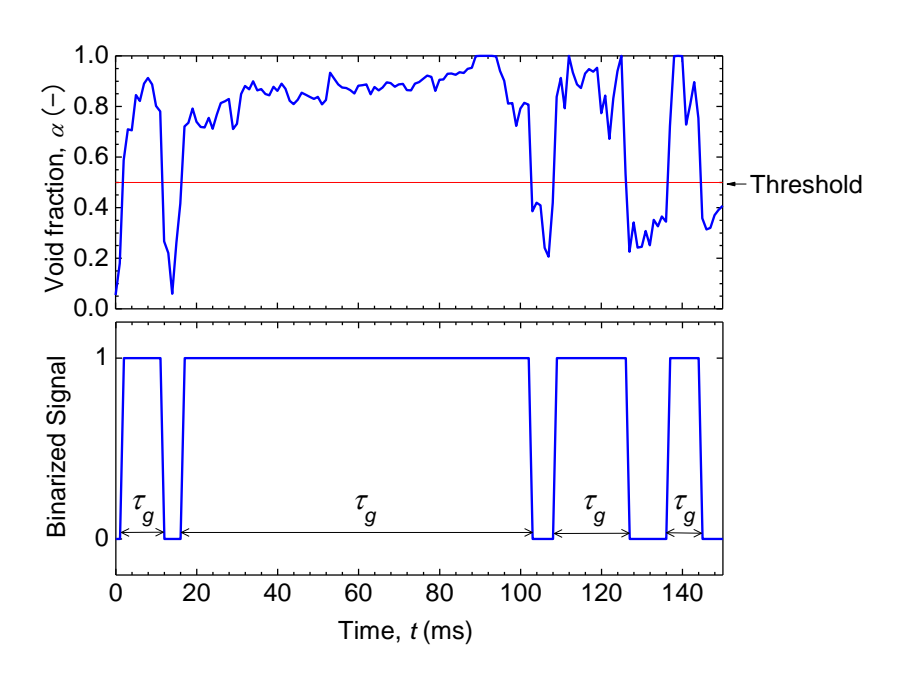


Figure 4 Evaluation of bubble residence time

2. Applicability of two-phase flow measurement using the 10×10 rod bundle geometry

The developed sensor was installed in the test section that simulates the 10×10 rod bundle; vertical upward two-phase flow in the rod bundle flow channel was evaluated in terms of three dimensional distributions of void fraction, phasic velocity and bubble chord length. Experimental results were compared to the existing results measured using a conductance probe in the rod bundle flow channel.

2.1 Air-water two-phase flow experiment

Figure 5 is a schematic of a REAL (REactor thermalhydraulics simulated by Air-water two-phase flow test Loop) facility. Figure 5(a) shows an overview of the REAL facility. The REAL facility mainly consists of a water circulation pump, an air compressor, an air receiver tank, an air-water separation tank, a heat exchanger, and test sections of a 10×10 rod bundle flow channel and large-diameter vertical pipe. In this experiment, the test section of a 10×10 rod bundle flow channel was used. Figure 5(b) shows the flow system of the REAL facility. The test fluid is water that has passed through an ion exchange resin. Water was supplied to the test section through the lower plenum by the circulating water pump. Air was supplied to the test section through the air receiver tank with the air compressor. The air receiver tank was used to control the inlet pressure alteration. In the downstream part of the test section, air and water were separated at the separation tank, the separated air was discharged into the atmosphere, and the separated water was recirculated to the water tank. The water temperature was controlled by the heat exchanger at 30 degrees Celcius. The water flow rate was measured by a magnetic flow meter (KEYENCE full-duplex-UH 100H), and was controlled by a regulating valve and bypass valve. The airflow rate was measured by 16 mass flow meters (Yamatake Co. LTD., MCF015), and it was controlled by the air supply system.

Figure 6 shows a schematic of the test section of the 10×10 rod bundle flow channel. In order to simulate the 10×10 rod bundle geometry, stainless-steel pipes with an outer diameter of 10mm were

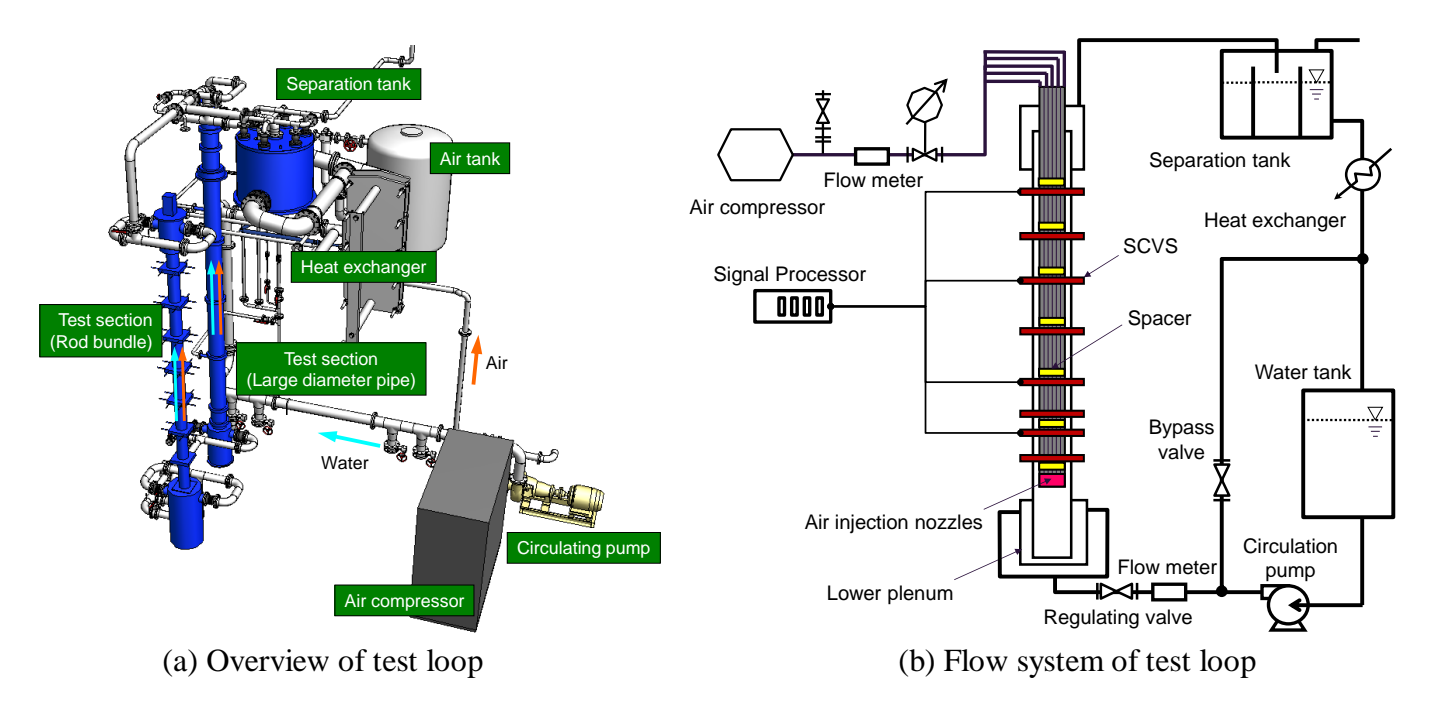


Figure 5 Schematic of REAL facility

The 14th International Topical Meeting on Nuclear Reactor Thermalhydraulics, NURETH-14 Toronto, Ontario, Canada, September 25-30, 2011

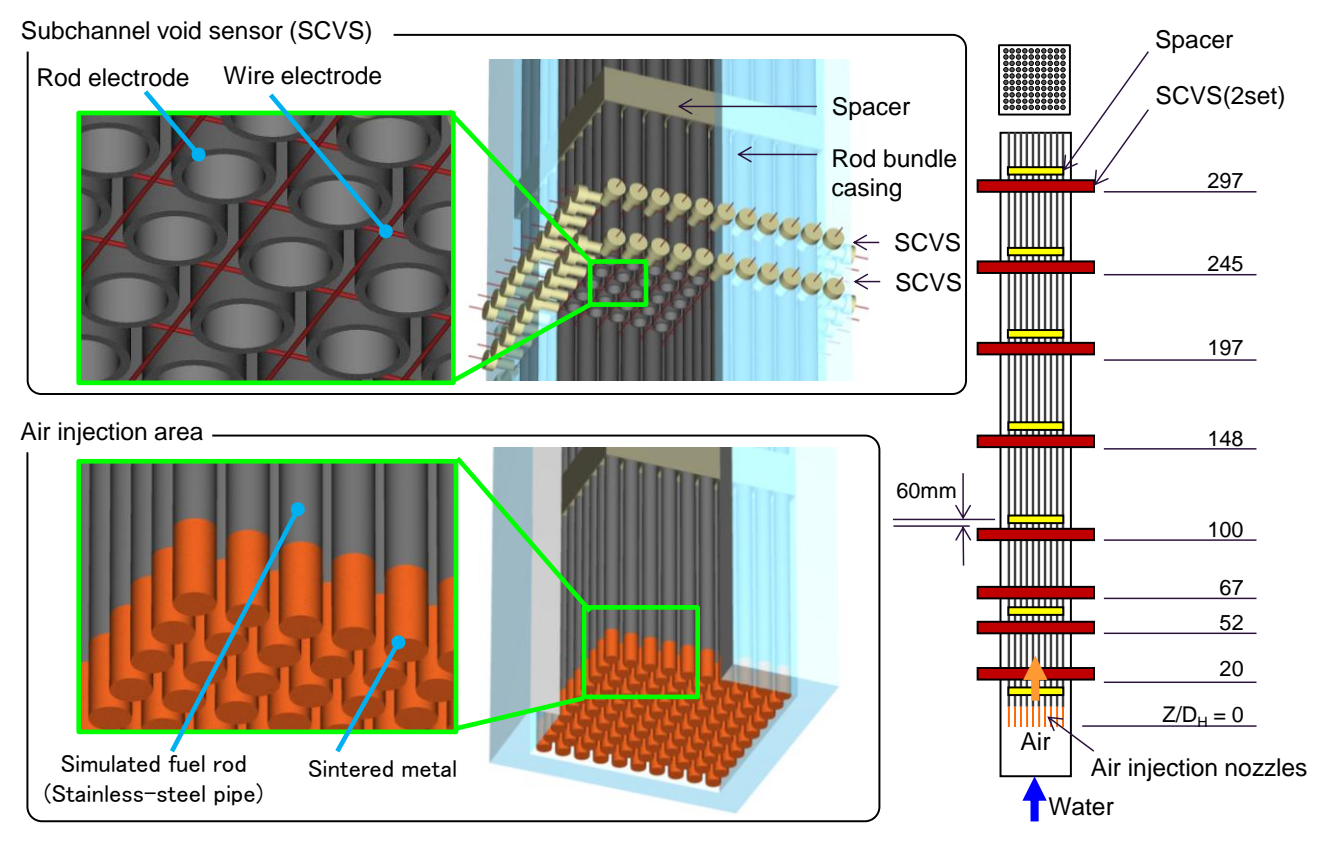


Figure 6 Cut-away view of test section

Table 1 Experimental conditions

Inlet superficial liquid velocity, j_L (m/s)	0.20, 0.50
Inlet superficial gas velocity, j_G (m/s)	0.23, 0.40, 0.61
Inlet gas flow distribution	Uniform, Annular
Sampling rate, f (frames/s)	1250
Measurement time, t (s)	25

arranged in a reticular pattern. The pitch of the rods was 13mm. The hydraulic diameter D_H was 10.6mm, and Z was the axial distance from the air injection nozzle. Grid spacers were installed in a total of seven positions, $Z/D_H = 14$, 62, 111, 159, 207, 256, and 304. Since the simulated fuel rods were used as independent electrodes, they were insulated by the spacers. The air injection nozzles were located at the bottom end of the rod bundle. In order to control the airflow rate at the inlet distribution, air can be supplied from the 10×10 injection nozzles. The air injection nozzles were made of sintered metal, which is exchangeable. In this experiment, the sieve mesh size of the sintered metal was 100 microns. Pairs of SCVS were located at a total of eight positions, $Z/D_H = 20$, 52, 67, 100, 148, 197, 245, and 297. A pair of sensors were placed 30 mm apart from each other, and 60mm apart from the spacer. Six pairs of the sensor ($Z/D_H = 52$, 100, 148, 197, 245, and 297) were located upstream of the spacer, and the others ($Z/D_H = 20$ and 67) were located downstream of it.

Table 1 shows the experimental conditions. The inlet superficial liquid velocity j_L was 0.20 and 0.50 m/s, and the inlet superficial gas velocity j_G was 0.37, 0.40 and 0.61 m/s. The inlet superficial velocity is defined as the superficial velocity at the air injection position ($Z/D_H = 0$). The airflow rate at the

inlet distribution was either uniform or annular. A uniform distribution of airflow rate means that air is supplied from all 100 nozzles at the same flow rate. An annular distribution of airflow rate means that air is supplied from only 36 nozzles located in the circumferential part of the rod bundle at the same flow rate. The sampling rate of SCVS was 1250 frames (cross sections) per second, and 25 seconds of time series data was acquired in each flow condition. The void fraction and the phasic velocity were evaluated as time-averaged distributions within 25 seconds. The phasic velocity was estimated based on the time lag between a pair of time series data that is 16 seconds long $(1250 \times 16 = 20000 \text{ points})$, which is estimated using a cross correlation function. The bubble chord length distribution is acquired by counting all the bubbles that pass the sensor in 25 seconds.

2.2 Comparison of two-phase flow measurement accuracy

The measurement principle of the developed SCVS is based on the same principles as that of the WMS system. Experimental results measured by the wire-mesh sensor were compared with other measurement techniques, such as conductance probe measurement and a high-speed X-ray tomography in order to evaluate measurement accuracy [9], [10]. The WMS has the same measurement accuracy as existing techniques. Therefore, this measurement has the same measurement accuracy in terms of signal-processing principle.

In order to compare the effect of the sensor geometry, the experimental results were compared to the existing experimental results in which Paranjape et al. have measured a vertical two-phase flow in 8×8 rod bundle flow channel with the conductance needle probe. Figure 7 shows comparisons of the void fraction and phasic velocity. The distance from the center of the flow channel x is normalized by a half width of the rod bundle casing W. The inlet distribution of the airflow rate is uniform. Solid symbols indicate this experiment, and the other symbols indicate the reference experiment. The measuring positions of this experiment and the reference experiment are $Z/D_H = 197$ and $Z/D_H = 200$, respectively. The hydraulics diameter of this experiment and the reference experiment were 10.6 mm and 14.8 mm. The inlet flow conditions of this experiment were $j_L = 0.20$ m/s, $j_G = 0.40$ m/s,

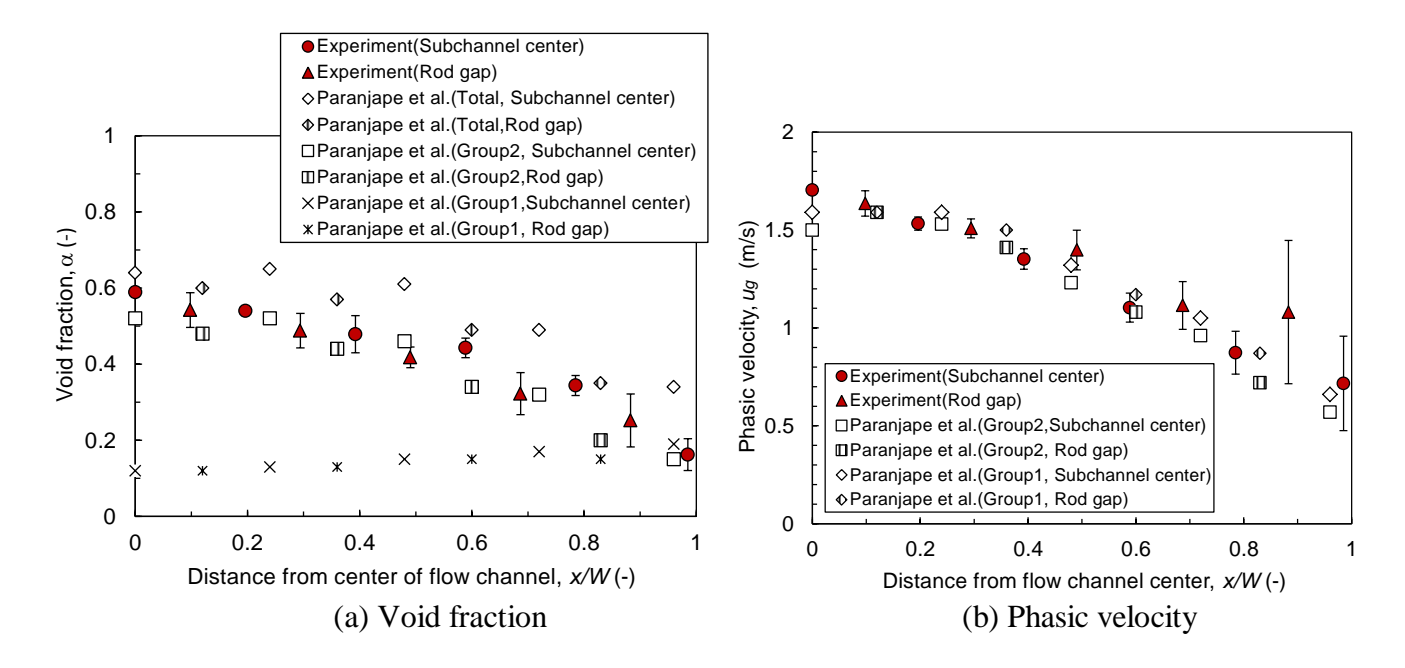


Figure 7 Comparison of measurement result between SCVS and conductance probe

however, the flow conditions at $Z/D_H = 197$ were $j_L = 0.20$ m/s and $j_G = 0.45$ m/s. The flow conditions of the reference experiment were $j_L = 0.2$ m/s, $j_G = 0.5$ m/s. As a result, two-phase flow in the rod bundle is almost the same profile. In this experiment, the void fraction and the phasic velocity are plotted as space-averaged values with an error bar of standard deviation. In the reference experiment, bubbles are classified into two groups according to the bubble size. Group 1 consists of spherical bubbles smaller than about 5mm. Group 2 consists of large bubbles of the type observed in slag or churn flow. Total void fraction without bubble classification is a sum of the void fraction of Group1 and Group 2. The void fraction acquired in this experiment was slightly below the value estimated from the reference experiment. In particular, the void fraction at the side wall and corner of the flow channel in this experiment was smaller than that of the reference experiment. The void fraction in this experiment may underestimate the existence of small bubbles shown as Group 1. The conductance probe used in the reference experiment is 50 microns in tip diameter. In contrast, since the electrode distance of SCVS was 1.5 or 2 mm, there is a possibility that the bubble detection sensitivity of SCVS is different from that of the probe. The phasic velocity distribution of this experiment was close to that of the reference experiment. At the side wall and corner of the flow channel, there was a significant secondary flow promoted by cross flow or pulsation flow. Since the phasic velocity was non-uniform in the circumferential region of the flow channel, the variation of spacial-averaged phasic velocity increases. The comparison results indicate that the developed sensor has almost the same accuracy as that used in the reference measurement technique. However, the effect of various flow conditions on the sensitivity characteristics of SCVS will be investigated and compared to the other measurement technique in the future.

2.3 Gas-liquid mixing process in 10×10 rod bundle flow channel

When air was supplied from the circumferential part of the air injection nozzles, three-dimensional distributions of the void fraction, phasic velocity and bubble chord length were evaluated by SCVS.

The representative results are shown in Figure 8 and 9. The distribution of void fraction, phasic velocity and bubble chord length are shown in each axial position Z/D_H =52, 100, 197 and 293. The time-averaged distribution of void fraction and phasic velocity are shown as a color map. Black parts of the color map indicate simulated fuel rods and the channel box. The bubble chord length distribution is normalized by the time-averaged void fraction, and is classified into the center part and circumferential part of the flow channel. The red line indicates the center part of the flow channel, and the blue line indicates the circumferential part of it.

The inlet flow conditions in Figure 8 are j_L =0.50 m/s and j_G = 0.23 m/s. At Z/D_H =52, and the peaks of the void fraction and phasic velocity are 0.37 and 1.1 m/s respectively in the circumferential part of the flow channel. In contrast, the void fraction in the center part of the flow channel is almost zero. Since bubbles hardly existed in the center part of the flow channel, the phasic velocity in the center of flow channel is also 0 m/s. Bubbles less than 20mm in bubble chord length mainly existed in the circumferential part of the flow channel. At Z/D_H =297, the void fraction and phasic velocity become homogeneous distributions except for the side wall and corner of the flow channel. The peaks of the void fraction and phasic velocity are 0.29 and 1.1 m/s respectively in the circumferential part of the flow channel. The bubble chord length distribution has a peak that is 3 mm long in each flow channel region. When air was injected the flow channel, bubbles less than 20 mm in bubble chord length mainly existed in each flow channel region. Some of the bubbles in the circumferential flow channel

moved to the center part of the flow channel, and the void fraction and phasic velocity distributions became almost homogeneous.

The inlet flow conditions in Figure 9 were $j_L = 0.50$ m/s and $j_G = 0.61$ m/s. At $Z/D_H = 52$, the peak of void fraction and phasic velocity were 0.42 and 1.6 m/s respectively in the circumferential part of the flow channel. Since the inlet superficial gas velocity was increased, both the void fraction and phasic velocity became high in the whole flow channel. However, the void fraction in the center of the flow channel was only 0.01. Bubbles with a chord length of less than 20mm mainly existed in the circumferential part of the flow channel, and there were no large bubbles that had up to 100 mm in bubble chord length. At $Z/D_H = 297$, the peaks of void fraction and phasic velocity were 0.61 and 2.6 m/s respectively in the center part of the flow channel. Most of the bubbles were concentrated on the center part of the flow channel. Large bubbles that were over 100 mm in bubble chord length were detected in the center of the flow channel. However, the peak of the bubble chord length distribution became less than 4 mm. When the gas superficial velocity was increased, the initial bubbles were not only coalesced and concentrated in the center of the flow channel, but also broken up by shared forces on the gas-liquid interface.

These experimental results suggest that the vertical air-water two-phase flow gas-liquid mixing process in rod bundle flow channel is evaluated as a three-dimensional distribution by SCVS.

3. Conclusion

A new void sensor that consists of 11-wire by 11-wire and 10-rod by 10-rod electrodes was developed for the 10×10 rod bundle geometry. The electrical potential in the proximity region between two wires provides the void fraction in the center subchannel region. Phasic velocity is estimated from the time lag between the pair of sensor signals. 121 points (= 11×11) of void fraction as well as those of phasic velocity can be measured. It is a characteristic of the devised sensor that the void fraction near the rod surface can be estimated by an electric potential in the proximity region between one wire and one rod. An additional 400 points of void fraction and phasic velocity can therefore be acquired in the 10×10 bundle. The time resolution of measurement is up to 1250 frames (cross sections) per second. In order to demonstrate the capability of the 10×10 rod bundle, the developed sensor was installed at 8 different height levels to acquire the two-phase flow dynamics along the axial direction. A pair of sensors was mounted in each level and placed 30 mm apart from each other to estimate the phasic velocity distribution on the basis of cross-correlation analysis. Experimental results were compared to the reference experiment measured with a conductance needle probe by Paranjape et al. The void fraction and phasic velocity distribution of the devised sensor provided almost the same results as those of the reference results. The sensors demonstrated the quasi three-dimensional flow structures, i.e. void fraction, phasic velocity and bubble chord length distributions.

The 14th International Topical Meeting on Nuclear Reactor Thermalhydraulics, NURETH-14 Toronto, Ontario, Canada, September 25-30, 2011

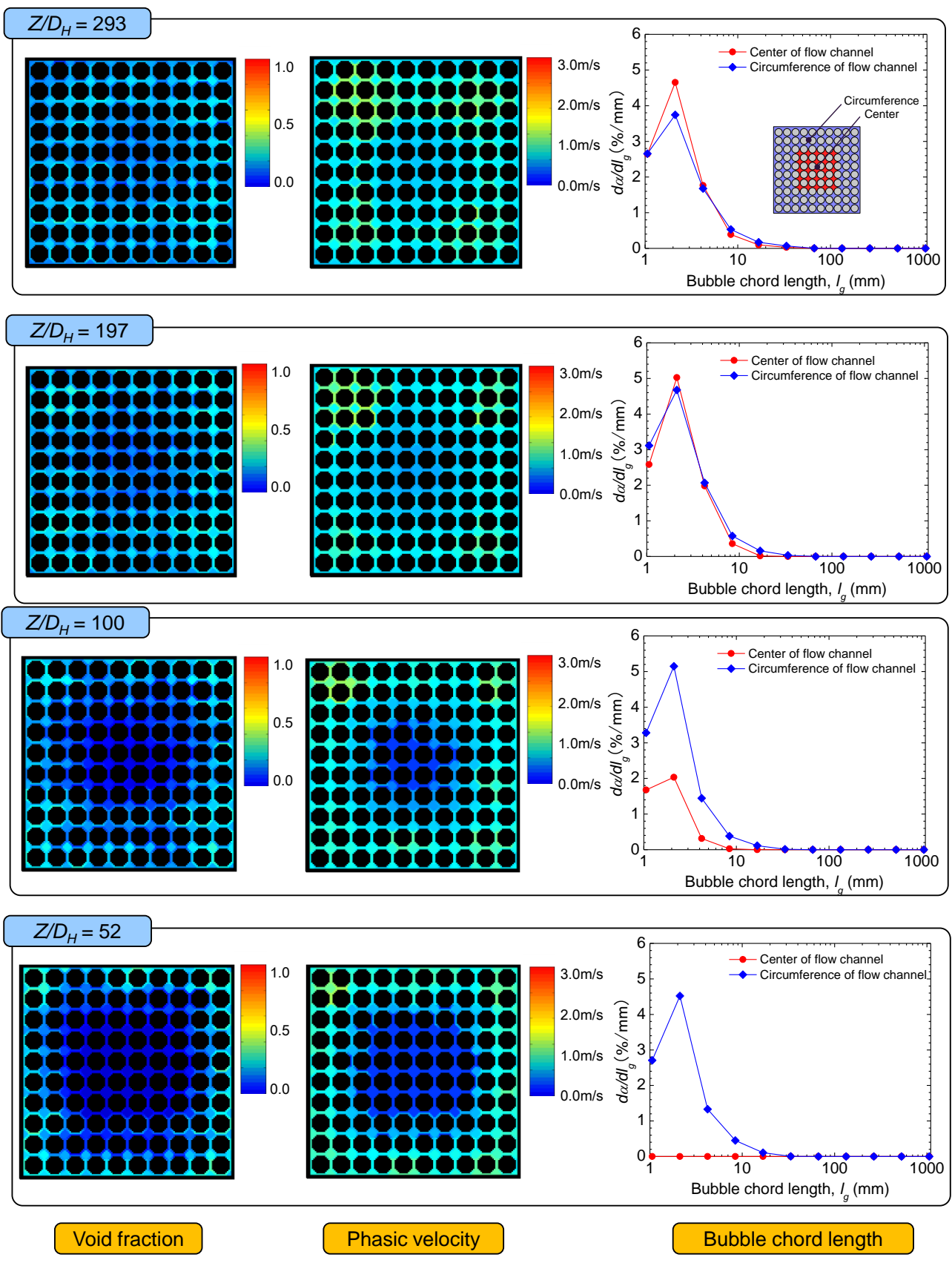


Figure 8 Void mixing process in the rod bundle flow channel ($j_L = 0.50$ m/s, $j_G = 0.23$ m/s, Inlet gas distribution: annular)

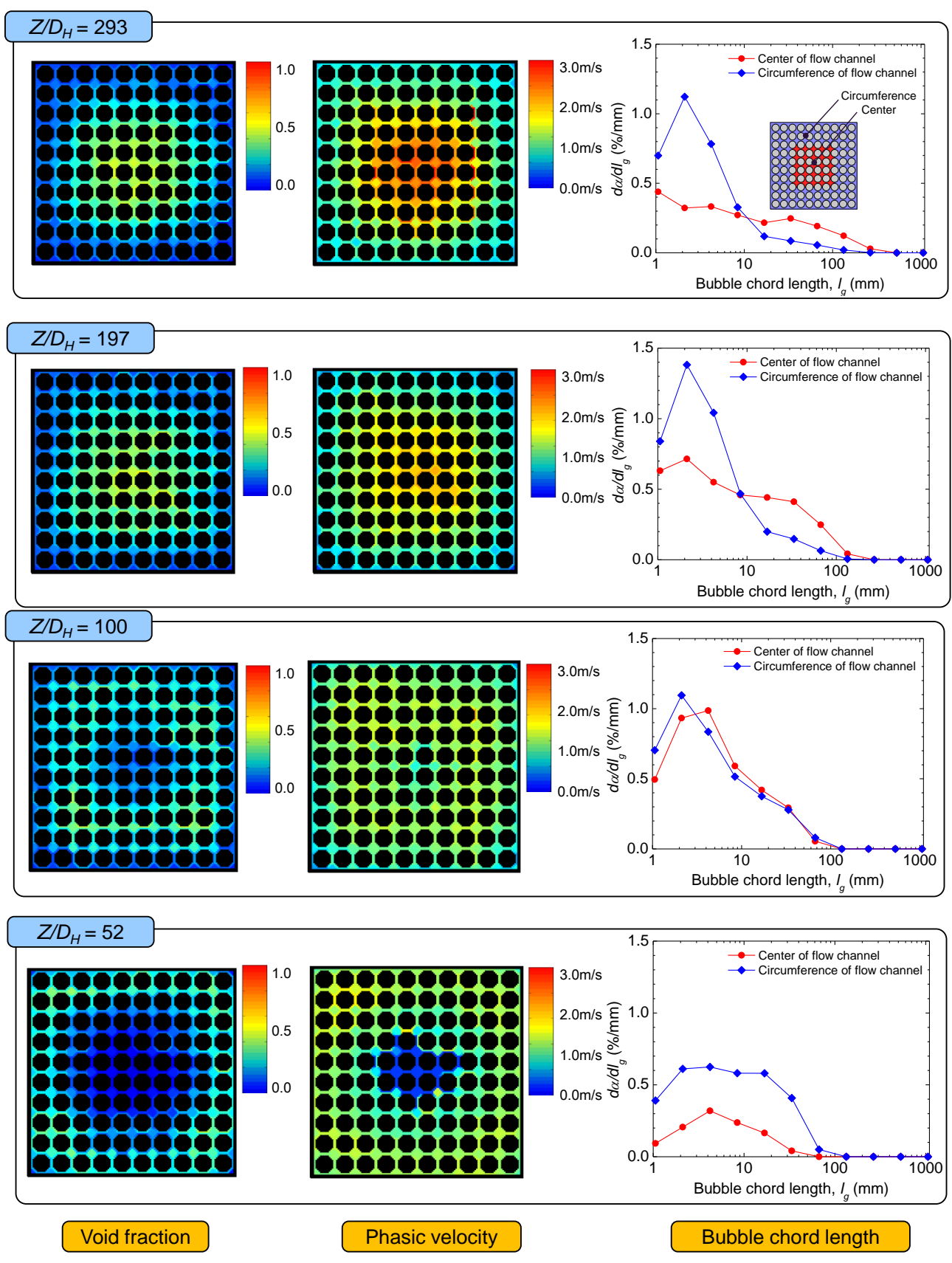


Figure 9 Void mixing process in the rod bundle flow channel ($j_L = 0.50$ m/s, $j_G = 0.61$ m/s, Inlet gas distribution: annular)

4. Acknowledgements

The authors would like to thank Professor H.-M. Prasser of ETH for his many helpful suggestions. They would also like to thank Takeo Yoshioka of CERES Inc. and Yoshiyuki Shiratori, Hirokazu Kamata and Kunihiko Nishiyama of Electric Power Engineering Systems Co., Ltd., for their assistance in these experiments.

5. References

- [1] M. Sadatomi, A. Kawahara, K. Kano, and S. Tanoue, "Flow characteristics in hydraulically equilibrium two-phase flows in a vertical 2×3 rod bundle channel", *International Journal of Multiphase Flow*, Vol. 30, 2004, pp. 1093-1119.
- [2] Y. Mizutani, S. Hosokawa, and A. Tomiyama, "Two-phase flow patterns in a four by four rod bundle", *Proceedings of the 14th International Conference on Nuclear Engineering*, Miami, Florida, USA, 2006 July 17-20.
- [3] S. Paranjape, M. Ishii, and T. Hibiki, "Modeling and measurement of interfacial area concentration in two-phase flow", *Nuclear Engineering and Design*, Vol. 240, 2010, pp. 2329-2337.
- [4] A. Inoue, T. Kurosu, T. Aoki, M. Yagi, T. Mitsutake, and S. Morooka, "Void fraction distribution in BWR fuel assembly and evaluation of subchannel code", *Journal of Nuclear Science and Technology*, Vol. 32, No. 7, 1995, pp. 629-640.
- [5] H.-M. Prasser, A. Bottger, and J. Zschau, "A new electrode-mesh tomograph for gas-liquid flows", *Flow Measurement and Instrumentation*, Vol. 9, 1998, pp. 111-119.
- [6] H.-M. Prasser, E. Krepper, and D. Lucas, "Evolution of the two-phase flow in a vertical tube decomposition of gas fraction profiles according to bubble size classes using wire-mesh sensors", *International Journal of Thermal Sciences*, Vol. 41, 2002, pp. 17-28.
- [7] H.-M. Prasser, "Evolution of interfacial area concentration in a vertical air-water flow measured by wire-mesh sensors", *Nuclear Engineering and Design*, Vol. 237, 2007, pp. 1608-1617.
- [8] H.-M. Prasser, M. Beyer, A. Bottger, H. Carl, D. Lucas, A. Schaffrath, P. Schutx, F.-P. Weiss, and J. Zschau, "Influence of the pipe diameter on the structure of the gas-liquid interface in a vertical two-phase pipe flow", *Nuclear Technology*, Vol. 152, 2005, pp. 3-22.
- [9] A. Manera, B. Ozar, S. Paranjape, M. Ishii, and H.-M. Prasser, "Comparison between wiremesh sensors and conductive needle-probes for measurements of two-phase flow parameters", *Nuclear Engineering and Design*, Vol. 239, 2009, pp. 1718-1724.
- [10] H.-H. Prasser, M. Misawa, and I. Tiseanu, "Comparison between wire-mesh sensor and ultrafast X-ray tomograph for an air-water flow in a vertical pipe", *Flow Measurement and Instrumentation*, Vol. 16, 2005, pp. 73-83.
- [11] H. Pietruske, and H.-M. Prasser, "Wire-mesh sonsors for high-resolving two-phase flow studies at high pressures and temperatures", *Flow Measurement and Instrumentation*, Vol. 18, 2007, pp. 87-94.